JOURNAL OF MATERIALS SCIENCE 29 (1994) 473–477

Quantitative microstructure maps for restrained directional growth

L. M. FABIETTI, J. A. SEKHAR
Department of Materials Science and Engineering, International Center for Micropyretics, University of Cincinnati, Cincinnati, OH 45221-0012, USA

Solidification morphology is affected by restraining the volume in which growth may occur. Such conditions occur during the solidification processing of composite materials. Microstructure maps are developed in this article to show the dominant fields of different morphologies which are expected during growth. Both wetting and non-wetting walls are considered. Tip temperatures of restrained solidification morphologies are additionally discussed.

1. Introduction

Solidification processing is an important manufacturing technique for the synthesis of materials. The type of process selected influences the morphology and size of the microstructure and properties displayed by the cast (solidified) part. Relationships between the characteristic length scales of the evolved solidification microstructures and the parameters of the governing process have been established by utilizing carefully designed experiments involving the solidification of pure materials and alloys [1–13]. Directional solidification of alloys has often been used as a reliable experimental method to establish such relationships between the solidification variables and the microstructural scales. Such experiments allow for independent control of the solidification variables which are the imposed solidification velocity (V), the temperature gradient (G) and the initial alloy composition (C_0) which control characteristic features of the solidification microstructures.

In a fibre composite material, the solidification process takes place in a restrained channel-like configuration [14–21]. The channels between the fibres may be of the order of magnitude of the primary spacing, the secondary arm spacing or the radius of curvature of a dendrite growing in the bulk. The channel size and the characteristics of the fibres are known to alter the morphologies and scales of microstructure from that obtained during unrestrained solidification. For example, the cellular morphology domains may be extended when measured as a function of the velocity [16, 19]. Similarly, an important microstructure modification is introduced by the dynamic contact angle relationship between the fibre and the matrix [19–21]. This last effect, usually ignored in bulk solidification, may be of importance in fibre composite solidification. Surface energy considerations have been shown to produce wetting and non-wetting dendrites. A typical example of a wetting and nonwetting dendrite is shown in Fig. 1. The dendrites in Fig. 1 were of an alloy of succinonitrile (SCN) and acetone, growing against wetting walls made of polytetrafluoroethylene (Teflon TFE) on the left side of the picture and against non-wetting walls made of perfluoro-ethylene-propylene (Teflon FEP) on the right side.

In this article, microstructure maps are generated to establish the dominant fields of various solidification morphologies noted during restrained growth. Both wetting and non-wetting surface are considered. In the microstructure maps, the dominant structure for a given combination of external velocity and channel size (assuming a fixed initial composition and thermal gradient) is identified.

2. Experimental procedure

Directional solidification experiments were carried out in the SCN–acetone system. The technique [22] and apparatus [23] have been described elsewhere. Two different type of glass cell were made with two 75 mm × 25 mm × 1 mm glass plates separated by 125 μm or 550 μm between which the SCN–acetone alloy was contained. The channels were built with Teflon strips with spacings ranging from 20 to 400 μm for the 125 μm cell. For the 550 μm cell, a capillary tube of 100 μm i.d. and 550 μm o.d. was placed between the glass plates. Fig. 2 shows schematic diagrams of a glass cell and an alloy cell growing in a channel. Only half of the glass cell was used for the channels. The other half was unrestricted and was used for a comparative study of the morphologies without the restraint. Two different types of Teflon were used for channel walls. One was Teflon TFE which produced a wetting effect with the solidifying material. The other was Teflon FEP and was used along with glass for the non-wetting channel wall. A calibrated thermocouple was inserted laterally in the cell to measure the interface temperature and to determine the alloy composition by the ring heater method [24].

Succinonitrile was distilled in a vacuum and then zone-refined (100 passes). The central part of the refining tube was transferred to a weighing bottle and

0022–2461

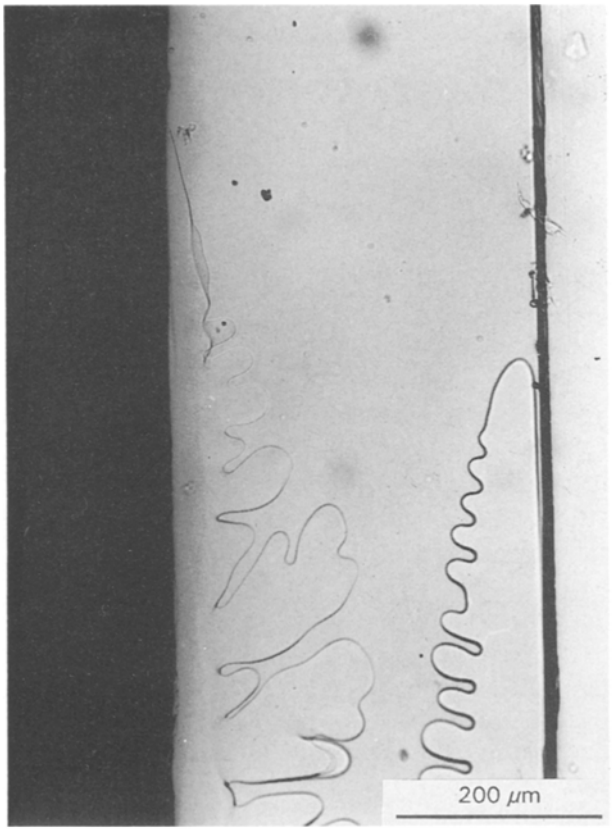

Figure 1 Dendrites in the SCN–acetone system growing against a wettable surface (Teflon TFE) on the left side of the picture and against a non-wettable surface (Teflon PFE) on the right side. $V = 5\,\mu m^{-1}\,s$, $G = 2.4\,K\,mm^{-1}$.

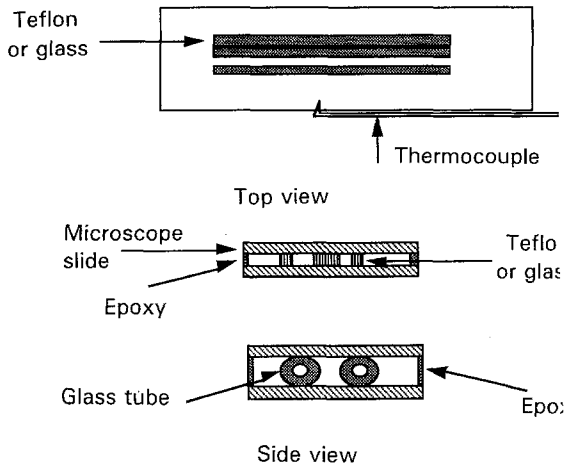

Figure 2 Schematic diagrams of the glass cell [19].

mixed with the calculated amount of high-purity acetone. A cell was then introduced into the bottle, allowing the alloy to fill the cell by capillarity. The operation of mixing the elements making up the alloy and the filling of the cell was carried out in a dry chamber to avoid any water contamination.

The experiments were carried out with the cells and dendrites aligned with the channel direction. The procedure was to run the glass cell for a predetermined duration at a velocity high enough to produce dendrites. If there was a mismatch between the dendrites and the channel directions, the sample was remelted and grown again until the desired orientation was achieved.

3. Results

3.1. Non-wetting walls

The channels built with Teflon strips had a rectangular shape. The height of the channel was fixed at 125 μm and the width was varied for each channel. In this article, for the development of the maps we analyse effects in the horizontal plane, i.e. in the plane containing the width of the channel. As explained above, special care was taken to have cells and dendrites aligned with the channel. Otherwise, half dendrites and half cells structures would appear as noted elsewhere [18]. Two microstructure maps are shown in Figs 3 and 4. In Fig. 3 the channels were made with glass tubes and the alloy composition was SCN–0.25 wt % acetone. It was noted that the cellular region expanded as a function of velocity due to the influence of the channel. The symmetry of the channel allows the growth of cells, dendrites and cellular dendrites. Cellular dendrites are cells with slight

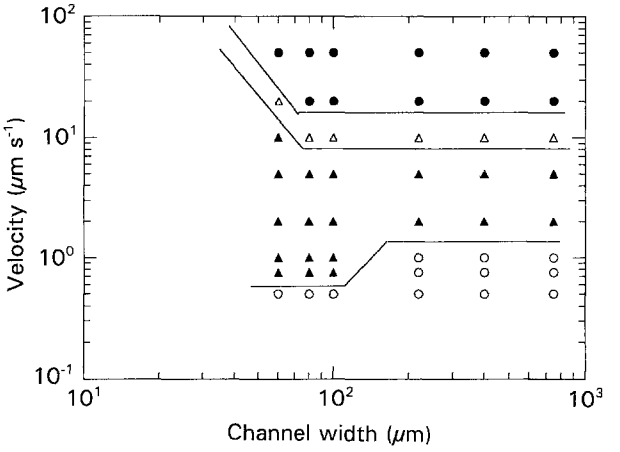

Figure 3 Microstructure map for SCN–0.3 wt % acetone alloy. Cylindrical geometry channel, non-wetting walls, temperature gradient $G = 4\,K\,mm^{-1}$. (○) Planar, (▲) cells, (△) cellular dendrites, (●) dendrites.

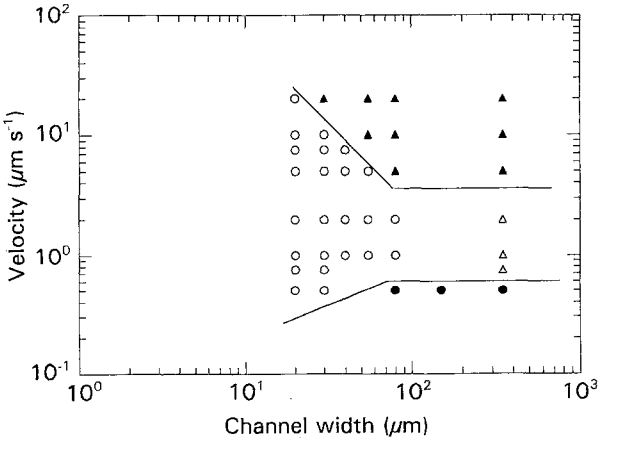

Figure 4 Microstructure map for SCN–0.5 wt % acetone alloy. Rectangular geometry channel, non-wetting walls, temperature gradient $G = 4\,K\,mm^{-1}$. (●) Planar, (○) cells, (△) cellular dendrites, (▲) dendrites.

tip perturbations but without the dendritic characteristics of fully developed side branches. For this alloy composition, the influence of the channel was noted to be negligible when the channel diameter was about 100 μm. Fig. 4 shows maps with the rectangular channels made with Teflon FEP. The alloy was SCN–0.5 wt % acetone. As before, the cell regime was noted to be expanded for small channel sizes. The map shows that increasing the channel spacing produces a transition from cell to cellular dendrite.

3.2. Wetting walls

Fig. 5 shows a microstructure map for SCN–1 wt % acetone alloy. The thermal gradient was $3\ \mathrm{K\,mm^{-1}}$. The main structures noted were the bi-cell and bi-dendrite morphologies. These bi-cells and bi-dendrites are solidification structures better defined by the schematic diagram in Fig. 6. Bi-cells have no side branches whereas bi-dendrites have side branches. The plot in Fig. 5 shows that for narrow channels the bi-cell mode has a smaller range of velocities than for wider channels. This occurs because of small differences between the channel walls which induce small differences in the rate of growth, causing one of the cells to take over from the other. A half-cell growing alone may have enough space to produce secondary arms and a half-dendrite is then produced. The half structure is produced because the channel walls are not entirely the same in terms of surface roughness. Due to the closeness of the walls, small differences in the growth conditions may cause one of the dendrites to eliminate the other, resulting in only one cell or dendrite. In such cases asymmetric solute segregation was obtained.

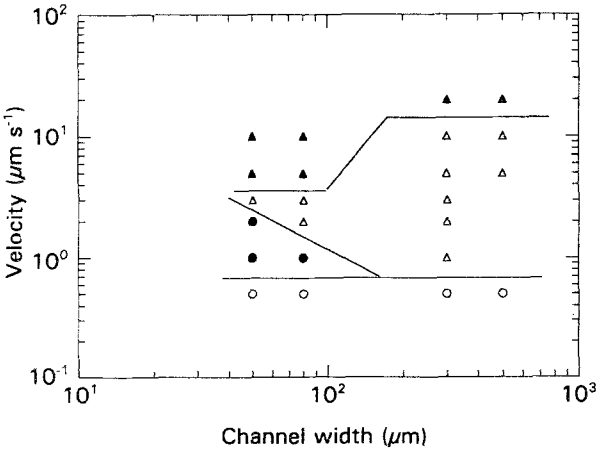

Figure 5 Microstructure map for SCN–1 wt % acetone alloy. Rectangular geometry channel, wetting walls, temperature gradient $G = 3\ \mathrm{K\,mm^{-1}}$. (○) Concave interface, (●) bi-cells, (△) bi-dendrites, (▲) dendrites.

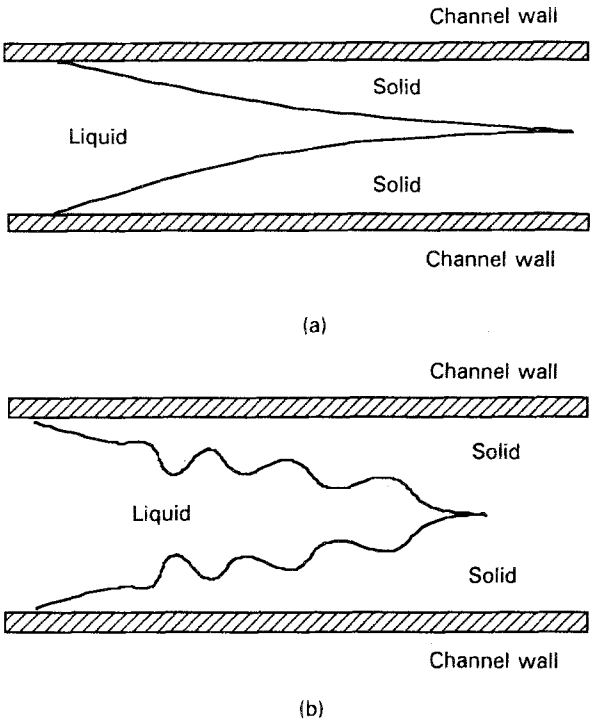

Figure 6 Schematic diagram of microstructures observed during the growth in channels with wetting walls: (a) bi-cell structure, (b) bi-dendrite structure. See Fabietti and Sekhar [19] for an actual picture of the microstructures.

4. Discussion

Solidification structures may be characterized by the tip temperature and the spacing of the growing morphology. For the case of restrained growth we discuss below the tip temperatures of dendrites growing against both wetting and non-wetting walls.

4.1 Non-wetting walls

The channel walls represent the physical condition of the equidistant plane between cells or dendrites, i.e. $\partial C/\partial x = 0$ where C is the liquid concentration and x is the direction perpendicular to the growth direction. When the channel size is different from the "natural" spacing there will be a mismatch between the actual boundary and the ideal one. This difference may introduce modifications in the interface morphology. Karma and Pelcé [25] have proposed a model for the cellular growth in a channel which reduces to two equations rearranged by Trivedi *et al.* [17]. These may be written as

$$d^2 = \left(\frac{\Gamma}{G}\right) V_c \left(\frac{50.8\Lambda}{2\Lambda - 1} - 47.93\right)\left(\frac{1 - (1 - k)\Lambda}{k[1 - (V_c/V)]}\right) \quad (1)$$

$$\frac{\Delta T}{\Delta T_0} = \frac{k\Lambda + (1 - \Lambda)(V_c/V)}{1 - (1 - k)\Lambda} \quad (2)$$

where d is the channel width, Γ the Gibbs–Thompson coefficient, G the gradient of temperature in the liquid at the interface, V_c the critical velocity for the onset of instability of a planar solid–liquid interface, V the external velocity, k the partition coefficient, ΔT the tip undercooling and ΔT_0 the solidification range of the alloy. Λ is a parameter defined [17] as the ratio of the cell width and the channel width. By solving the system of equations we eliminate the parameter Λ and calculate the undercooling as a function of the channel spacing for a fixed velocity, or as a function of the velocity for a fixed channel spacing. Fig. 7 shows a comparison with the experimental results for the SCN–acetone system. Note that the agreement is good at high velocities but only reasonable at low velocities.

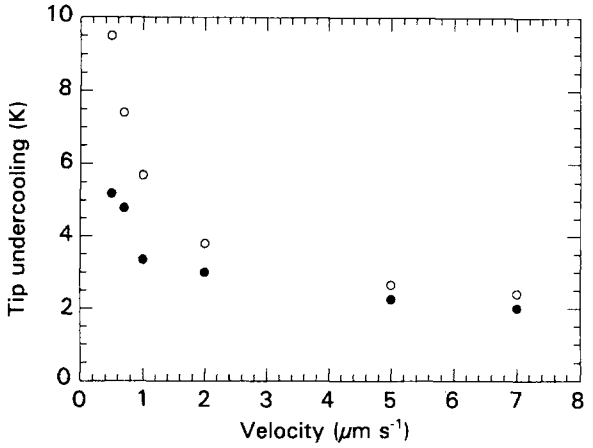

Figure 7 Tip undercooling as a function of velocity for a cell growing inside a 60 μm diameter channel. Non-wetting walls, SCN–0.3 wt % acetone, temperature gradient $G = 4\ \mathrm{K\,mm^{-1}}$. (●) Experimental data, (○) model of Karma and Pelce [25].

In non-wetting channels the contact angle between the walls and the interface has no decisive influence except when the channel is very small, i.e. of the same order of magnitude as the radius of curvature for a dendrite growing under similar experimental conditions [16, 19]. The principal modification in these channels is on account of the build-up of solute caused by the closeness of the fibres. The magnitude of the interaction between the channel and the growing morphology is controlled by the relative size of the channel and the primary spacing. When the channel size is smaller than the primary spacing, the solute will build up at the walls and thus decrease the solute gradient. This effect has a stabilizing influence on the perturbations generated in the cellular regime close to the dendrite transition. Consequently, cells grow in a range of velocities larger than the range of the cellular growth in bulk materials.

Cells grow following the heat flow direction, but dendrites have crystallographic preferences which may produce a tilt in the growth direction when the cell approaches the limit of the velocity of the cell-to-dendrite transition [19]. If there is a misalignment between the channel direction and the preferred crystallographic direction, pseudo half-cells and half-dendrites have been observed [18], "pseudo" because the tip is not really at the restraint interface but in the liquid. If the misalignment between the channel and the dendrites is severe, a confused structure is produced [16, 19]. If the channel width is between one and two primary spacings, the morphology will depend on the particular growth condition. If the morphology is a perfectly centred cell inside the channel, it will tend to destabilize the interface because the solute gradient is higher than the gradient which would be obtained at the "natural" boundary. If the morphology is dendritic, the diffusion field close to the tip is not affected and no change in the morphology is expected. For channels bigger than two spacings the mismatch may modify the solute field of a cell or dendrite growing close to the walls. The change in the growth conditions for one of the cells or dendrites may induce changes in the rest of them growing inside the same channel. Steady-state growth may not be achieved under such conditions.

4.2. Wetting walls

For the wetting condition the contact angle controls the microstructure over a large range of velocities [19,20]. When the velocity is low enough to give a planar interface in the bulk, the tendency of the matrix material to grow on the walls will produce a concave (towards the liquid) interface. When the velocity is increased, the growth against the wall is enhanced and bi-cells and bi-dendrites are formed [19]. The wetting affects the secondary arm spacing and the tip temperature [19]. If tertiary arms are produced, there is a strong possibility for a bulk dendrite to take over from the dendrites growing against the wall because the tip temperature of the wall dendrites will have a sharper decrease with velocity than the bulk dendrites when the velocity is increased [19]. The wetting effect also influences the dendritic growth direction [19, 20]. In general, the microstructure in the channel will be highly positively segregated at the centre line for the condition when the partition coefficient $k < 1$. The tip temperatures for wetting dendrites are a function of velocity, composition and the contact angle. No theory is currently available to describe this temperature adequately. However, experimental observations [19, 20] have shown that the velocity dependence of wetting dendrite tip temperature is different from that of non-wetting dendrites [19, 20].

5. Summary

Quantitative microstructure maps for composite growth are shown for the first time for the case of cells and dendrites growing within wetting and non-wetting channels. These microstructure maps are shown for the case when the dendrite direction is aligned with the channel direction during directional growth.

Acknowledgement

The work was carried out as part of grant AFOSR-90-0308 monitored by Dr Alan Rosenstein.

References

1. W. A. TILLER, K. A. JACKSON, J. W. RUTTER, and B. CHALMERS, *Acta Metall.* **1,** (1953) 428.
2. W. W. MULLINS and R. F. SEKERKA, *J. Appl. Phys.* **35,** (1964) 444.
3. W. KURZ and D. J. FISHER, *Acta. Metals.* **18,** (1970) 287.
4. M. H. BURDEN and J. D. HUNT, *J. Cryst. Growth* **22,** (1974) 99.
5. *Idem. ibid.* **22,** (1974) 109.
6. M. E. GLICKSMAN, R. J. SCHAEFER and J. D. AYERS, *Met. Trans.* **7A, (1976)** 1747.
7. R. K. TRIVEDI and W. A. TILLER, *Acta Metall.* **26,** (1978) 671.
8. *Idem, ibid.* **26,** (1978) 679.
9. R. K. TRIVEDI, *J. Cryst. Growth* **49,** (1980) 219.
10. S. C. HUANG and M. E. GLICKSMAN, *Acta Metall* **29,** (1981) 701.
11. *Idem, ibid.* **29,** (1981) 717.

12. R. TRIVEDI and K. SOMBOONSUK, *Mater. Sci. Eng.* **65,** (1984) 65.
13. K. SOMBOONSUK and R. K. TRIVEDI, *Acta Metall.* **6,** (1985) 1051.
14. A. MORTENSEN, J. A. CORNIE and M. C. FLEMINGS, *Metal. Trans.* **19A,** (1988) 709.
15. *Idem, J. Met.* **60,** (1988) 12.
16. J. A. SEKHAR and R. TRIVEDI, *Mater. Sci. Eng.* **A114,** (1989) 133.
17. R. K. TRIVEDI, S. HAN and J. A. SEKHAR, in "Solidification of Metal-Matrix Composites", edited by P. Rohatgi, (Metallurgical Society Warrendale, Pennsylvania, 1990) p. 23.
18. J. A. SEKHAR and R. TRIVEDI, *Mater Sci. Eng.* **A114,** (1991) 9.
19. L. M. FABIETTI and J. A. SEKHAR, in "Nature and Properties of Semi-Solid Materials", edited by J. A. Sekhar and J. A. Dantzig (Metallurgical Society, Warrendale, Pennsylvania, 1992) p. 41.
20. *Idem. J. Mater. Res.* **7,** (1992) 1987.
21. *Idem, Met. Trans.* **23A,** (1992) 3361.
22. J. D. HUNT, K. A. JACKSON and H. BROWN, *Rev. Sci. Instr.* **27,** (1966) 805.
23. J. T. MASON and M. A. ESHELMAN, *Report IS*-4906 (Ames Laboratory, Ames, Iowa, 1986).
24. H. ESAKA, PhD thesis, Ecole Polytechnique Federal de Lausanne (1986).
25. A. KARMA and P. PELCE, *Phys. Rev.* **A39** (1989) 4162.

Received 5 January
and accepted 28 July 1993